On the Equations of Dynamics of a Roller Seismic Isolation Bearing

Ibrakhim Mirzaev[1, 2, a)], Djumaev Khikmatulla[1, b)], Malikjon Turdiev[1, c)], Jakhongir Shomurodov[3, d)] and Rakhmatov Nodirbek[4. e)]

[1]*Tashkent State Transport University, Tashkent, Uzbekistan*
[2]*Institute of Mechanics and Seismic Stability of Structures named after M.T. Urazbaev of the Academy of Sciences of the Republic of Uzbekistan*
[3]*Renessance Education University, Tashkent, Uzbekistan*
[4]*National University of Uzbekistan, Tashkent, Uzbekistan.*

[a)] Corresponding author: ibrakhim.mir@mail.ru
[b)] djumaev1959@mail.ru
[c)] malikjon_ts@mail.ru
[d)] jakhongir_shf@mail.ru
[e)] nodirbekrakhmatov0@gmail.com

Abstract. An analysis of publications on the dynamics of roller sliders revealed inaccuracies in the construction of mathematical models for describing dynamic processes. In research, the law of motion of the lower plate is usually specified, and the motion of the upper plate must be determined by solving a dynamic problem. In structural dynamics problems involving sliding friction forces, the direction of the friction force was determined by the difference in the velocities of the rubbing elements, and the stick-slip mode requires solving a nonlinear problem using a special method. A thorough analysis of the processes in roller sliders has shown that the start of the relative motion of the plates and the start of their joint motion as a solid body cannot be realized solely by the sign function of the difference in the velocities of the upper and lower plates. The plates begin to roll relative to each other only when the inertial force exceeds the sum of all forces acting in the horizontal direction. A stick-slip mode is also possible during the movement process. Graphs of changes in time of displacements, velocities, and accelerations of the upper plate and specified movements of the lower plate are given according to analytical functions and records of real earthquakes. The presence of a sufficiently long horizontal plane in the middle of the lower plate increases the effectiveness of the seismic isolator.

INTRODUCTION

Seismic isolation in modern construction is considered an important technology for improving the seismic resistance of buildings. In recent years, numerous studies have been conducted in this field, including theoretical foundations, experimental work, and new technological solutions.

In the article [1] sets the task of evaluating the effectiveness of seismic isolation technologies for buildings. The scientific novelty of the research lies in the fact that the work systematically analyzes the historical development and practical experience of applying isolation methods, as well as justifies new directions for future research—three-dimensional isolation and protection of non-structural elements.

In the articles [2, 3] is devoted to reducing the impact of earthquakes on buildings using seismic isolation. The aim of the study is to evaluate the effectiveness of various types of isolators and determine their potential for use in earthquake-prone areas. Theoretical analysis and computer modeling were used as the main methods. The authors consider devices such as elastomeric supports, movable supports, and friction isolators. The results showed that these systems effectively reduce earthquake energy. In conclusion, it is emphasized that the work creates an important scientific basis for improving seismic safety in construction practice.

In the article [4] examines the effectiveness of seismic isolation devices in buildings prone to earthquakes. The main objective of the work is to compare different isolation methods and determine their impact on the seismic safety of structures. To solve the problem, calculation methods and computer modeling were used to evaluate the dynamic response of buildings under various types of seismic impacts. The authors use friction devices, elastomeric bearings, and sliding supports to analyze the behavior of structures. The results show that isolation significantly reduces stresses in buildings and increases their stability. However, it was noted that in some models, changes in the friction coefficient and plastic properties of materials were not fully taken into account, which is a limitation of the study.

In the article [5] discusses various types of seismic isolators and their role in ensuring the seismic resistance of structures. The aim of the work is to conduct a comparative analysis of rubber isolators, friction devices, and movable supports, identifying their advantages and disadvantages. To solve the problem, the author uses a review of the literature and experimental observations. The results show that elastomeric isolators are most effective at reducing vibrations, friction devices are simple and inexpensive, and movable supports significantly increase the seismic safety of buildings. However, changes in the friction coefficient over time and issues of durability remain insufficiently studied.

In the article [6] examines the concept of seismic isolation and current trends in its development. The main objective is to evaluate the effectiveness of various types of isolators and determine their application in construction. To solve the problem, the author uses theoretical analysis and the results of previous experimental studies. The paper compares the characteristics of elastomeric supports, friction-based devices, and sliding isolators. The results show that such systems significantly reduce building vibrations during seismic events.

In the article [7] investigates the dynamics of multi-mass systems under multi-point seismic excitation. Modeling showed a significant influence of different excitation points on the response of the structure. The work is particularly important for bridges and high-rise buildings. The study considers various seismic scenarios and analyzes the characteristics of structural vibrations. No specific type of seismic isolators was used in the work; the behavior of the structure was studied within the framework of a general dynamic model.

In the article [8] raises the issue of optimal design of inertial vibration dampers. Using a multi-criteria optimization method, the authors determined the parameters of an effective device. The results show that such devices effectively reduce vibrations in multi-story buildings. The paper proposes a new approach to the design of seismic protection equipment.

In the article [9] theoretically and experimentally studies the effectiveness of roller isolators. In the study, the results of computer modeling were compared with laboratory experiments. It was shown that the device significantly reduces seismic vibrations. At the same time, the need for accurate selection of isolator parameters is emphasized.

In [10], the technical report is devoted to the principles of operation of roller insulators for bridges. Operational parameters and areas of application are considered. The effectiveness of the device for road bridges is confirmed.

In the article [11] examines a roller isolator with an additional energy dissipation element. Experiments have shown higher stability compared to conventional isolators. The system provides reliable seismic protection. These achievements pave the way for the introduction of new devices into construction practice.

In the article [12] discusses the use of dry friction devices for seismic isolation of turbine units at nuclear power plants. The authors performed numerical calculations of various design parameters and evaluated the effectiveness of the system. The results showed that dry friction elements significantly reduce the amplitude of vibrations and increase the stability of the turbine unit. The optimal operating modes of the isolator were also identified. However, the need for more extensive experimental testing in real conditions before practical implementation is emphasized.

In the article [13] investigates the influence of the horizontal gap between the foundation and the sliding grillage structure on building vibrations during an earthquake. Using mathematical modeling and numerical calculations, the authors analyzed changes in dynamic characteristics as the gap size increased. The results showed that choosing the optimal gap size significantly increases the seismic resistance of the building. The paper substantiates the importance of considering the location and dimensions of structural elements when designing seismic protection. The main drawback is that the conclusions are largely based on a theoretical model and require additional confirmation by experimental testing.

In the article [14] investigates the problem of experimentally determining the dynamic coefficient of dry friction according to Amontons-Coulomb. The authors developed a special laboratory device and a method for measuring the coefficient of friction under various loads and surface conditions. The results show that the dynamic coefficient of dry friction is more than twice as small as the static coefficient. The study emphasizes the need to take real coefficients into account when calculating oscillatory systems and seismic isolation devices. The main advantage of the work is the practical focus and novelty of the measurement method. However, since the experiments were conducted only under limited conditions, additional experimental studies are required to generalize the results.

In the article [15] evaluates the effectiveness of TLCD and TMD devices for buildings, taking into account the interaction between the structure and the ground. The optimal parameters for the devices are determined. This work is important for improving the seismic resistance of buildings.

In the article [16] is devoted to the theoretical foundations of earthquake-resistant construction and structural dynamics. Mathematical models and analytical solutions have been developed. The work serves as a methodological basis in seismology.

In the article [17] is devoted to wave processes in underground pipelines when interacting with soil. A bilinear model was used for numerical analysis. The high sensitivity of pipelines to earthquakes was established.

In article [18], a new type of seismic isolation device with inclined multi-roller supports was developed and tested to protect important equipment and structures from the effects of earthquakes. The results of the study show that such devices are effective and stable. However, dynamic calculations did not fully account for some nonlinear effects of plastic deformation of the material and variability of the friction coefficient. The effectiveness of the device is considered using the example of a specific type of equipment and structures, but additional research is needed for application to other objects.

In article [19], numerical modeling of buildings with friction pendulum supports demonstrated their effectiveness in reducing vibrations. The main parameters were taken into account, but nonlinear effects were not fully investigated. The work contributes to the development of seismic protection systems.

The monograph [20] technical report contains a comprehensive assessment of modern seismic isolation devices. Experimental data and theoretical models are compared. Practical recommendations for their use in construction are provided.

The overall goal of all the above-mentioned work is to improve the seismic safety of buildings and reduce the impact of earthquakes through the use of seismic isolation technologies. Achievements include the combination of theoretical models with experimental results, the development of new types of devices, and confirmation of their effectiveness. At the same time, a number of shortcomings remain. Many studies have been conducted in laboratory conditions or based on theoretical models, which limits the scope of their practical application.

In conclusion, it can be noted that existing studies comprehensively cover the theoretical, practical, and technological aspects of seismic isolation. The results obtained make a significant contribution to ensuring the seismic resistance of buildings, but in the future, field tests, cost reduction of technologies, and the development of solutions to protect non-structural elements will be required.

This paper introduces the conditions for the start of relative motion of seismic isolator plates, as well as the conditions for their joint motion as a solid body. Equations of motion are proposed depending on the ratio of the absolute values of the velocities of the upper and lower plates of the seismic isolator. The proposed equations of motion are applicable in the absence of sliding friction.

MATERIAL AND METHODS

To facilitate understanding of the dynamics of roller seismic isolators, let us examine the case of flat plates undergoing horizontal motion only. Fig. 1 shows a schematic view of a roller isolation device with flat plates. Let us consider the equation of motion of the upper plate with mass m, given the motion of the lower plate u_2 under the action of an earthquake. Since the mass of the cylinder is negligible compared to the mass of the upper plate, the rotational inertia of the cylinder is neglected. The upper plate receives force through the movement of the lower plate. If the lower plate moves as a result of an earthquake, the upper plate is set in motion by the force arising at the contacts of the plates with the cylinder. Let's introduce the symbols $\mu_1 = \delta_1/r$ и $\mu_1 = \delta_2/r$, where δ_1, δ_2-coefficients of rolling friction between the cylinder and the upper and lower plates, respectively, r – radius of the cylinder.

Let the plates begin to move together first. Then the conditions for the movement of the upper u_1 and lower plates apply in the absence of relative movement between them.

$$\ddot{u}_1 = \ddot{u}_2, \dot{u}_1 = \dot{u}_2, u_1 = u_2 - \Delta u. \quad (1)$$

Here, Δu represents the relative displacement of the upper plate at the moment of transition from relative motion to joint motion as an absolute rigid body, Δu=0 at the initial moment of the process.

At the moment when the acceleration reaches the value necessary to overcome the rolling friction forces at the contacts between the cylinder and the upper and lower plates, the plates will begin to move relative to each other. At this moment, the speed of the upper plate is equal to the speed of the lower plate, and the displacement of the upper plate is determined by the ratio (1).

$$|\ddot{u}_2| > (\mu_1 + \mu_2) \cdot g. \quad (2)$$

During the movement of the plates, condition $|\dot{u}_1| \geq |\dot{u}_2|$ may occur, in which case the upper plate rotates the cylinder, so the resistance forces at the cylinder contacts are added together. Then the equation of motion of the upper plate is as follows

$$\ddot{u}_1 = \text{sign}(\dot{u}_1 - \dot{u}_2)(\mu_1 + \mu_2) \cdot g. \quad (3)$$

If $|\dot{u}_1| < |\dot{u}_2|$ occurs, the upper plate is moved by the rolling friction force at the contact point between the upper plate and the cylinder.

$$\ddot{u}_1 = \text{sign}(\dot{u}_1 - \dot{u}_2)\mu_1 \cdot g. \quad (4)$$

If $|\dot{u}_1 - \dot{u}_2| < \varepsilon$ and $|\ddot{u}_2 - \ddot{u}_1| < (\mu_1 + \mu_1) \cdot g$, where ε - a small positive number, the value of which is selected depending on the time step size in step-by-step problem solving. In this case, the plates begin to move together and the process is determined by the ratio (1).

Where μ_1, μ_2 - olling friction coefficients at the contacts between the cylinder and the upper and lower plates, respectively.

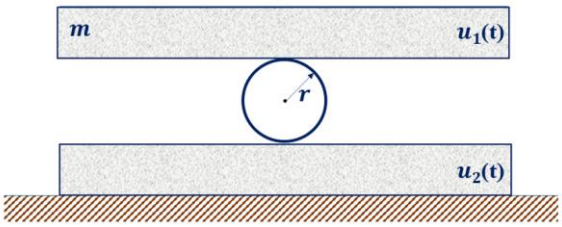

FIGURE 1. Schematic representation of a roller insulation device with flat plates

Now let us consider the problem for a roller insulation device with a V-shaped bottom plate with a horizontal section in the middle and an angle of inclination φ (Fig. 2). If the center of the bottom base is a plane with length l (Fig. 2), then the following relationship holds for equations (5) - (8).

$$\phi = \{0, |u_r - u_2| \leq l/2\,| \quad \text{or } \phi = \left\{0, \left|\frac{u_1 - u_2}{2}\right| \leq l/2\right| \quad ,$$

where φ_0 – this angle of inclination in the bottom plate, $u_r = (u_1 + u_2)/2$ – displacement of the cylinder center at small φ.

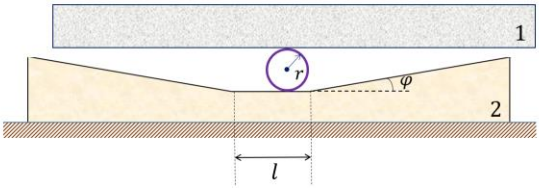

FIGURE 2. Schematic representation of a roller insulation device for a plate with a V-shaped bottom plate with a horizontal section in the middle and an angle of inclination φ.

In this case, too, in the absence of relative motion of the plates, relations (1) hold. Unlike flat plates, the condition for the onset of relative motion of the plates is given by

$$|\ddot{u}_2| > |\text{sign}(\dot{u}_1 - \dot{u}_2)\mu_1(g + \text{sign}(u_r - u_2)\ddot{u}_2\text{tg}\phi) + \text{sign}(\dot{u}_1 - \dot{u}_2)\mu_2(g + \text{sign}(u_r - u_2)\ddot{u}_2\text{tg}\phi)\cos\phi - \\ -\text{sign}(u_1 - u_2)\tfrac{1}{2}(g + \text{sign}(u_r - u_2)\ddot{u}_2\text{tg}\phi)\sin 2\phi|. \quad (5)$$

Accordingly, for $|\dot{u}_1| \geq |\dot{u}_2|$, the equation of motion of the upper plate is

$$\ddot{u}_1 = \text{sign}(\dot{u}_1 - \dot{u}_2)\mu_1(g + \text{sign}(u_r - u_2)\ddot{u}_2\text{tg}\phi) + \text{sign}(\dot{u}_1 - \dot{u}_2)\mu_2(g + \text{sign}(u_r - u_2)\ddot{u}_2\text{tg}\phi)\cos\phi - \\ -\text{sign}(u_1 - u_2)\tfrac{1}{2}(g + \text{sign}(u_r - u_2)\ddot{u}_2\text{tg}\phi)\sin 2\phi, \quad (6)$$

otherwise

$$\ddot{u}_1 = \text{sign}(\dot{u}_1 - \dot{u}_2)\mu_1(g + \text{sign}(u_r - u_2)\ddot{u}_2\text{tg}\phi) - \text{sign}(u_1 - u_2)\tfrac{1}{2}(g + \text{sign}(u_r - u_2)\ddot{u}_2\text{tg}\phi)\sin 2\phi. \quad (7)$$

In both equations, the initial conditions for the transition from one state to another at time $t=t^*$ are: $u_1 = u_1(t\ )$, $\dot{u}_1 = \dot{u}_1(t\ )$, and at the beginning of the relative motion of the upper plate we have $\dot{u}_1 = \dot{u}_2$, $u_1 = u_2 - \Delta u$.

If, during the movement of the plates, the difference in their velocities is close to zero and the difference in accelerations is less than the resistance forces

$$|\dot{u}_1 - \dot{u}_2| < \varepsilon,$$

and

$$|\ddot{u}_2 - \ddot{u}_1| = |\text{sign}(\dot{u}_1 - \dot{u}_2)\mu_1(g + \text{sign}(u_r - u_2)\ddot{u}_2\text{tg}\phi) + \text{sign}(\dot{u}_1 - \dot{u}_2)\mu_2(g + \text{sign}(u_r - u_2)\ddot{u}_2\text{tg}\phi)\cos(\phi) - \\ -\text{sign}(u_1 - u_2)\frac{1}{2}(g + \text{sign}(u_r - u_2)\ddot{u}_2\text{tg}\phi)\sin 2\phi|, \quad (8)$$

then the plates begin to move together and the process is determined by the ratio (1).

RESULTS AND DISCUSSION

First, let us present the results calculated based on the values μ_1=0.055, μ_2=0.054, φ=0˚, i.e., for flat plates. Let the motion of the lower plate be defined as follows:

$$u_2 = \left\{\frac{\text{At}}{t_0}\sin(\omega t), t \le t_0\right|$$

In this case, the maximum displacement amplitude of the lower base is A=0.1 m, the circular oscillation frequency is ω=2π *rad/s* and t_0=6 s.

Figure 4 shows graphs of the displacements, velocities, and accelerations of the upper and lower plates over a period of 15 seconds. In this case $|u_1|_{max}$=0.026 m, u_{2max}=0.1 m, $|v_1|_{max}$=0.16 *m/s*, v_{2max}=0.62 *m/s*, w_{1max}=1.08 m/s^2, w_{2max}=3.91 m/s^2. The results show that the maximum displacement values differ by a factor of 3.8, the maximum velocity values by a factor of 3.9, and the maximum acceleration values by a factor of 3.6.

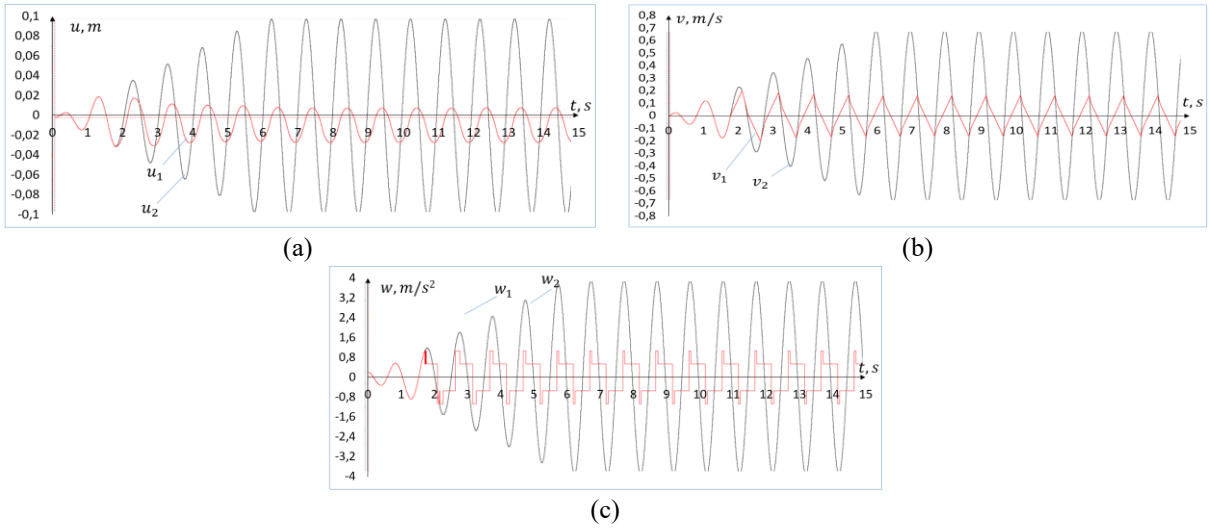

(a) (b) (c)

FIGURE 3. Displacements (a), velocities (b), and accelerations (c) of the upper (1) and lower (2) plates.

Figure 3 shows when $|\dot{u}_1| \ge |\dot{u}_2|$ acceleration w_1 is determined by the rolling friction forces acting on the contacts between the cylinder and the upper and lower plates.

Figure 4 shows the results of calculations for lower rolling friction coefficients, i.e., μ_1=0.023, μ_2=0.024. In this case $|u_1|_{max}$=0.001 m, u_{2max}=0.1 m, $|v_1|_{max}$=0.06 *m/s*, v_{2max}=0.62 *m/s*, w_{1max}=0.43 m/s^2, w_{2max}=3.91 m/s^2. The results show that the maximum displacement values differ by a factor of 10, the maximum velocity values by a factor of 10.3, and the maximum acceleration values by a factor of 9.8.

Figures 3 and 4 show that as the rolling friction coefficients decrease, the maximum values of displacement, velocity, and acceleration of the upper plate are significantly reduced.

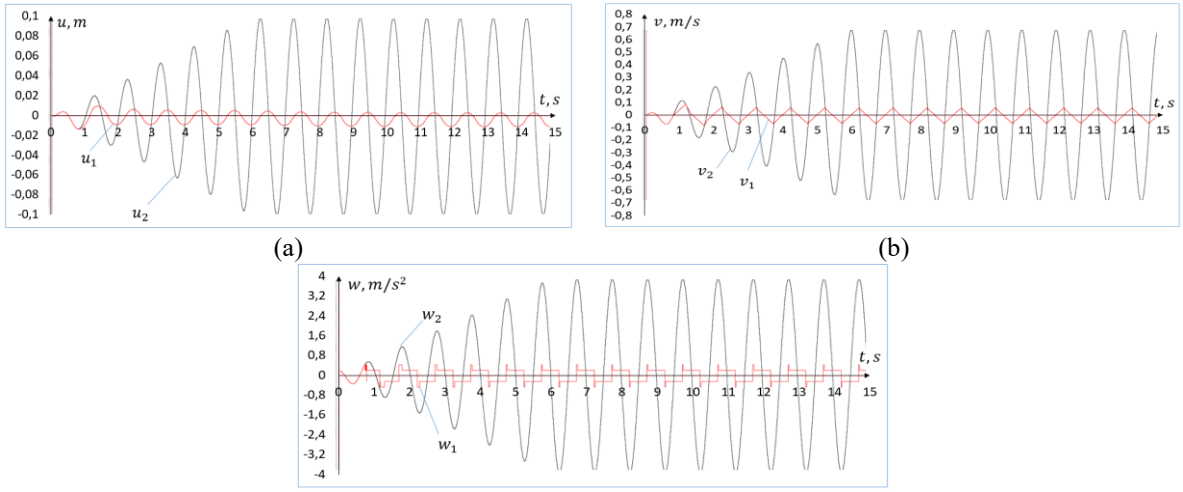

FIGURE 4. Displacements (a), velocities (b), and accelerations (c) of the upper (1) and lower (2) plates.

Figures 5 and 6 show the results of calculations with a V-shaped bottom plate at φ=5° with a horizontal section in the middle l=0.02 m.

Figure 5 shows the results for a rolling friction coefficient of μ_1=0.055, μ_2=0.054. In this case $|u_1|_{max}$=0.03 m, u_{2max}=0.1 m, $|v_1|_{max}$=0.17 m/s, v_{2max}=0.62 m/s, w_{1max}=1.38 m/s^2, w_{2max}=3.91 m/s^2. The results show that the maximum displacement values differ by a factor of 3.3, the maximum velocity values by a factor of 3.6, and the maximum acceleration values by a factor of 2.8. The V-shaped lower plate causes additional resistance to relative movement, which reduces the effectiveness of the seismic isolator.

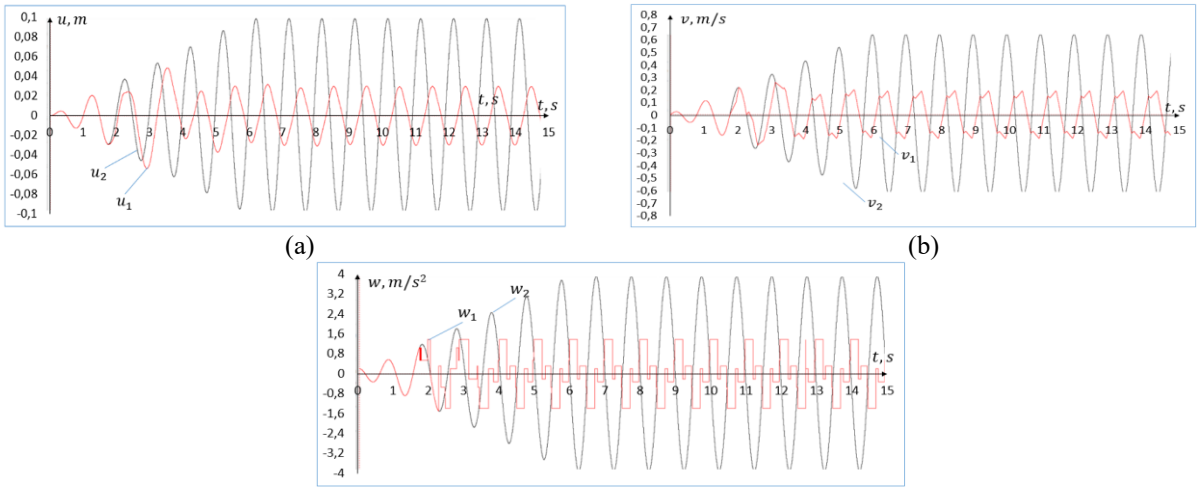

FIGURE 5. Displacements (a), velocities (b), and accelerations (c) of the upper (1) and lower (2) plates at μ_1=0.055, μ_2=0.054.

Figure 6 shows the results of calculations for rolling friction coefficients μ_1=0.023, μ_2=0.024. In this case $|u_1|_{max}$=0.03 m, u_{2max}=0.1 m, $|v_1|_{max}$=0.19 m/s, v_{2max}=0.62 m/s, w_{1max}=1.05 m/s^2, w_{2max}=3.91 m/s^2. The results show that the maximum displacement values differ by a factor of 3.3, the maximum velocity values by a factor of 3.3, and the maximum acceleration values by a factor of 3.7. The results show that in this case, the maximum values of the speed and acceleration of the upper plate decrease significantly as the friction coefficient decreases, but there are no significant changes in the maximum displacement values.

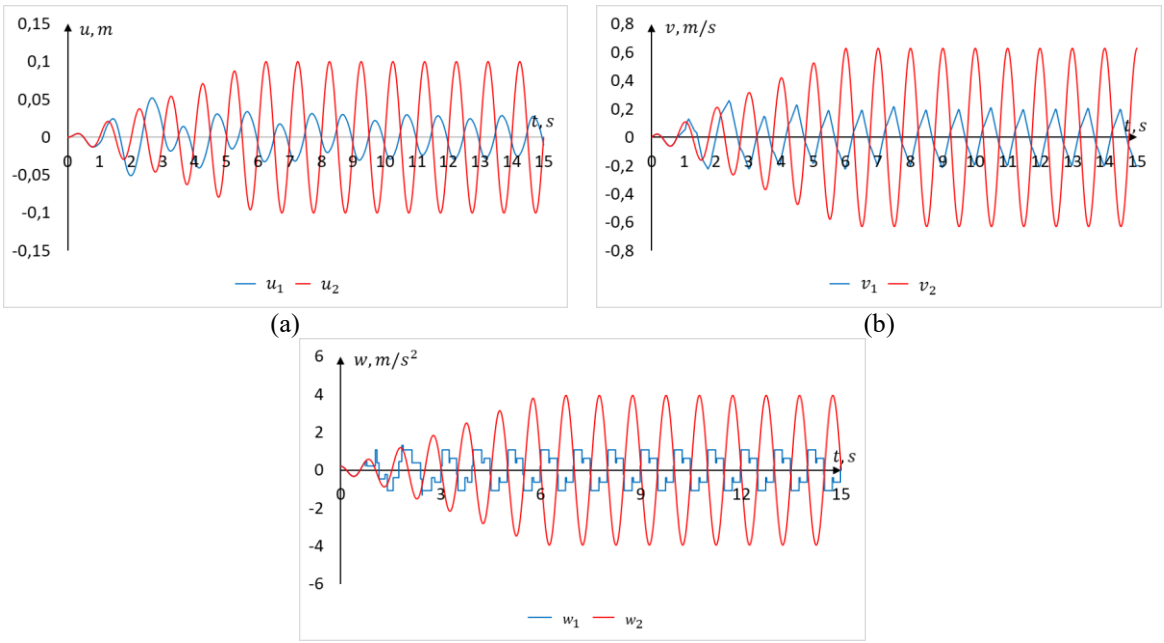

FIGURE 6. Displacements (a), velocities (b), and accelerations (c) of the upper (1) and lower (2) plates at μ_1=0.023, μ_2=0.024.

Figure 7 shows the results of calculations for μ_1=0.055, μ_2=0.054 и φ=10˚. In this case $|u_1|_{max}$=0.05 *m*, u_{2max}=0.1 *m*, $|v_1|_{max}$=0.37 *m/s*, v_{2max}=0.62 *m/s*, w_{1max}=2.21 *m/s²*, w_{2max}=3.91 *m/s²*. The results show that the maximum displacement values differ by a factor of 2, the maximum velocity values by a factor of 1.6, and the maximum acceleration values by a factor of 1.8. The results show that as the angle of inclination increases, the maximum displacement, velocity, and acceleration values of the upper plate increase proportionally.

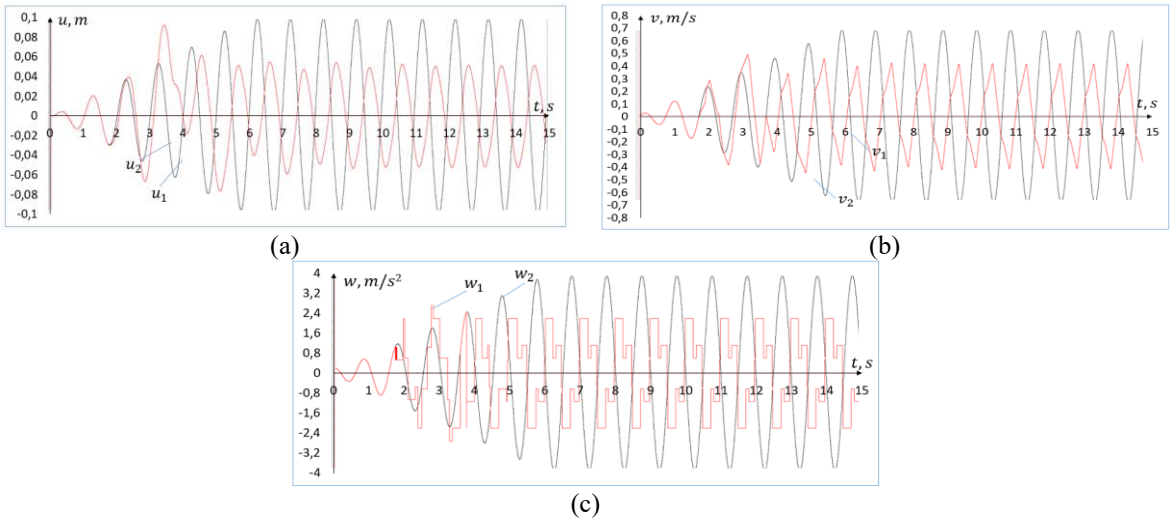

FIGURE 7. Displacements (a), velocities (b), and accelerations (c) of the upper (1) and lower (2) plates at μ_1=0.055, μ_2=0.054 and φ=10˚.

Now let's look at the results calculated based on records of actual earthquakes. We will perform the calculations with μ_1=0.055 and μ_2=0.054.

Figures 8 and 9 for the Nocera Umbra 2 earthquake, Italy – 000856 (03.04.1998, 9 points on the MSK-64 scale, maximum acceleration – 3.73 *m/s²*, maximum displacement – 0.0054 *m*, digitization step – 0.005 *s*, duration – 40.990 *s*) the results of the calculations are given. In this case u_{1max}=0.0019 *m*, u_{2max}=0.0054 *m*, v_{1max}=0.038 *m/s*,

v_{2max}=0.11 *m/s*, w_{1max}=1.05 *m/s*^{2}, w_{2max}=3.73 *m/s*^{2}. The results show that at φ=5˚, the maximum displacement values differ by a factor of 2.8, the maximum velocity values by a factor of 2.8, and the maximum acceleration values by a factor of 3.6.

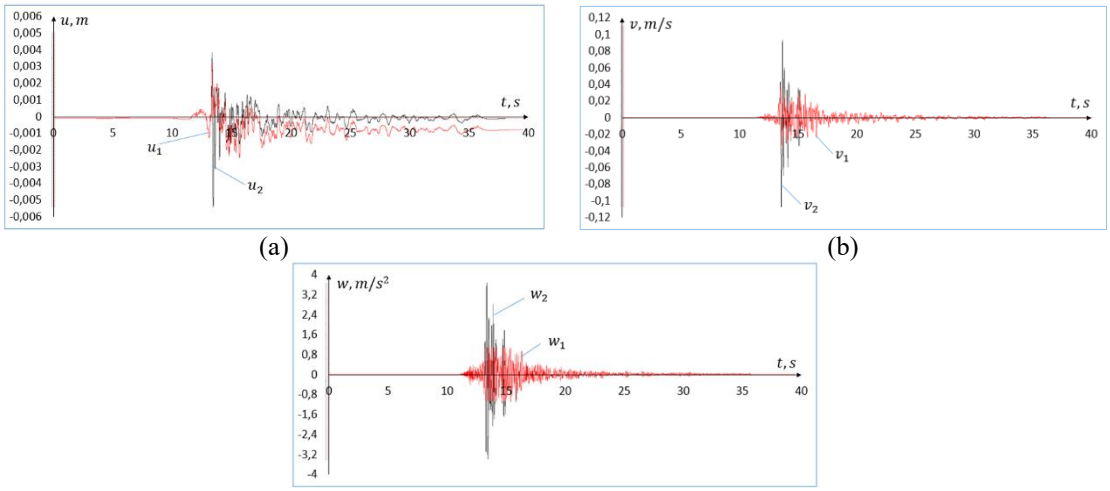

(a) (b)

(c)

FIGURE 8. Displacements (a), velocities (b), and accelerations (c) of the upper (1) and lower (2) plates at φ=5˚, *l*=0.02 *m*.

For a clear analysis of the dynamics of the upper plate, Fig. 9 shows the displacement of the plates in the time interval 13-15 s. It can be seen that in the 2-second time interval, the processes of relative and joint motion are observed several times. As a result of the acceleration amplitude reaching high values, the displacement and velocities also reach their maximum values during this time period.

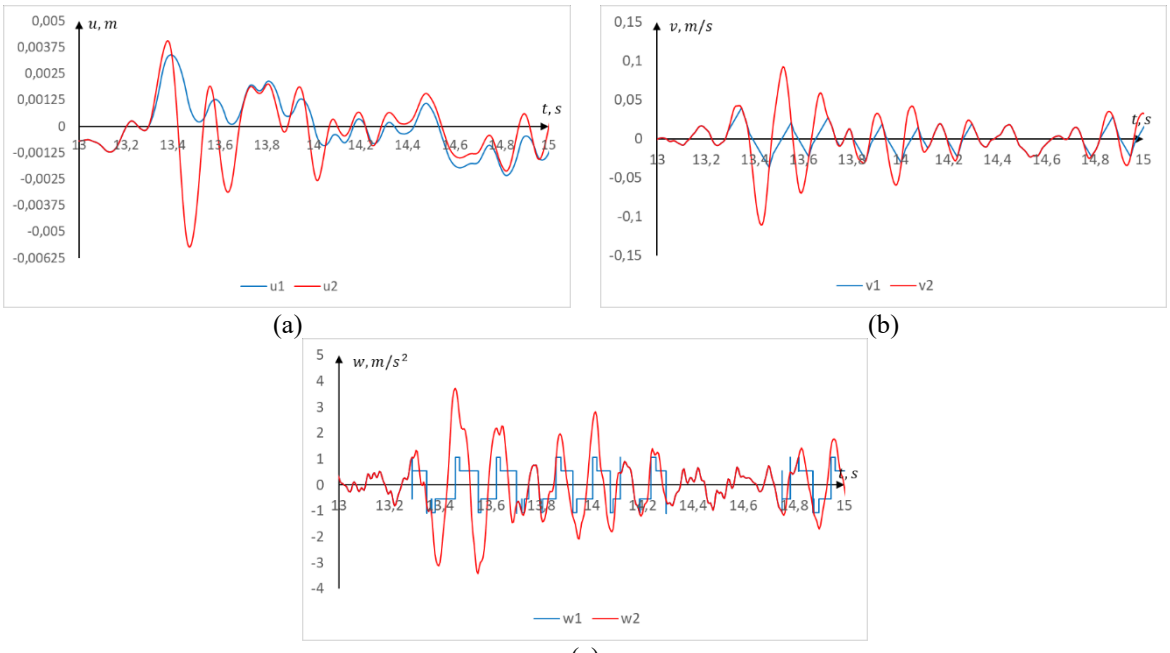

(a) (b)

(c)

FIGURE 9. Displacements (a), velocities (b), and accelerations (c) of the upper (1) and lower (2) plates at φ=5˚, *l*=0.02 *m*.

In this case, it can also be seen from the acceleration graphs that in situations where $|\dot{u}_1| \geq |\dot{u}_2|$, the acceleration values of the upper plate increase due to the action of two rolling friction forces.

Figures 10 and 11 show the Tabas earthquake, Iran – 000187 (September 16, 1978, 10 points on the MSK-64 scale, maximum acceleration – 10.17 *m/s*^{2}, maximum displacement – 0.3446 *m*, digitization step – 0.005 *s*, duration

– 78.395 *s*), the results of the calculations are shown. At φ=5˚, the following results were obtained u_{1max}=0.34 *m*, u_{2max}=0.34 *m*, v_{1max}=0.39 *m/s*, v_{2max}=0.87 *m/s*, w_{1max}=1.93 *m/s*^{2}, w_{2max}=10.17 *m/s*^{2}. The results show that at φ=5˚, the maximum displacement values do not differ, the maximum velocity values differ by a factor of 2.2, and the maximum acceleration values differ by a factor of 5.3.

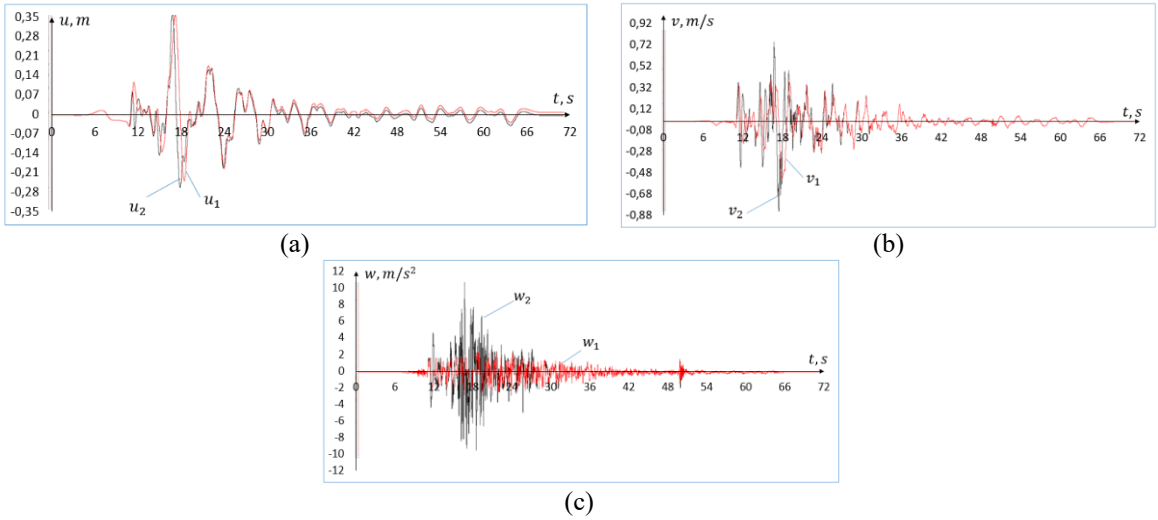

FIGURE 10. Displacements (a), velocities (b), and accelerations (c) of the upper (1) and lower (2) plates at φ=5˚, *l*=0.02 *m*.

Figure 11 shows the results obtained at φ=0˚. In this case u_{1max}=0.19 *m*, u_{2max}=0.34 *m*, v_{1max}=0.38 *m/s*, v_{2max}=0.87 *m/s*, w_{1max}=1.04 *m/s*^{2}, w_{2max}=10.17 *m/s*^{2}. The results show that the maximum displacement values differ by a factor of 1.8, the maximum velocity values by a factor of 2.3, and the maximum acceleration values by a factor of 9.8.

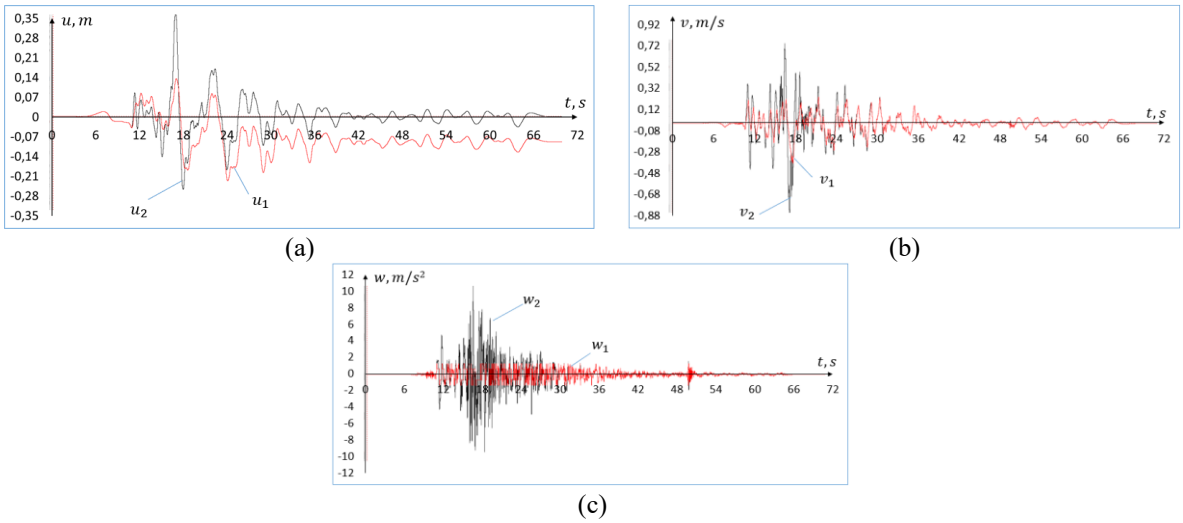

FIGURE 11. Displacements (a), velocities (b), and accelerations (c) of the upper (1) and lower (2) plates at φ=0˚, *l*=0.02 *m*.

Figures 12 and 13 show the Tolmezzo earthquake, Italy – 000055 (May 6, 1976, 9 points on the MSK-64 scale, maximum acceleration – 3.35 *m/s*^{2}, maximum displacement – 0.029 *m*, digitization step –0.005 *s*, duration – 46.535 *s*), the results of the calculations are shown.

Figure 12 shows the results obtained for φ=5˚ and *l*=0.02 *m*. In this case u_{1max}=0.028 *m*, u_{2max}=0.029 *m*, v_{1max}=0.18 *m/s*, v_{2max}=0.2 *m/s*, w_{1max}=1.93 *m/s*^{2}, w_{2max}=3.35 *m/s*^{2}. The results show that the maximum displacement values differ by a factor of 1.03, the maximum velocity values by a factor of 1.1, and the maximum acceleration values by a factor of 1.7.

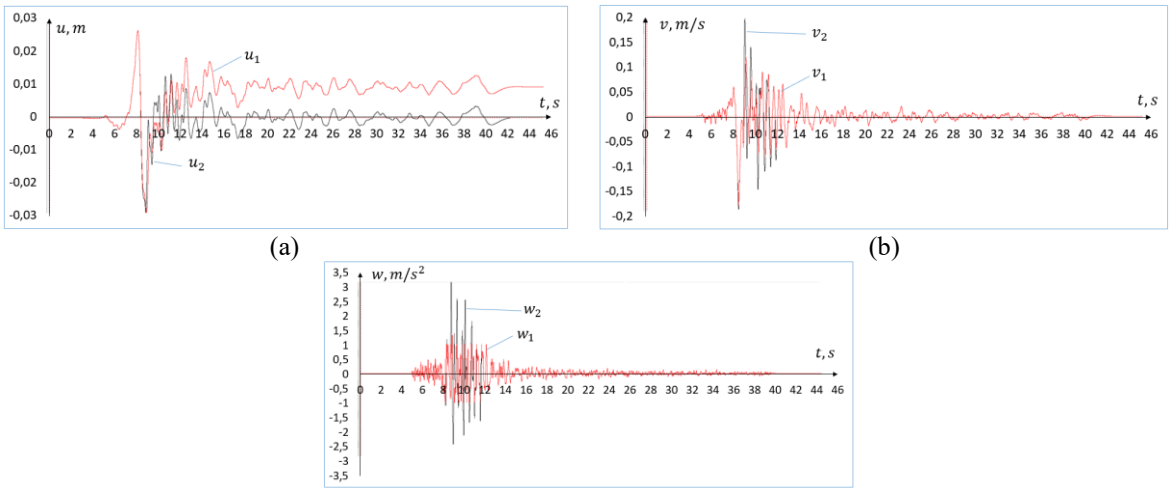

FIGURE 12. Displacements (a), velocities (b), and accelerations (c) of the upper (1) and lower (2) plates at φ=5˚, l=0.02 m.

Figure 13 shows the results obtained for φ=5˚ and l=0.01 m. In this case u_{1max}=0.028 m, u_{2max}=0.029 m, v_{1max}=0.18 m/s, v_{2max}=0.2 m/s, w_{1max}=1.36 m/s^2, w_{2max}=3.35 m/s^2. The results show that the maximum displacement values differ by a factor of 1.03, the maximum velocity values by a factor of 1.1, and the maximum acceleration values by a factor of 2.5. The residual displacement after t=12 s does not exceed 0.005 m, and the parameter l allows the residual displacement to be controlled.

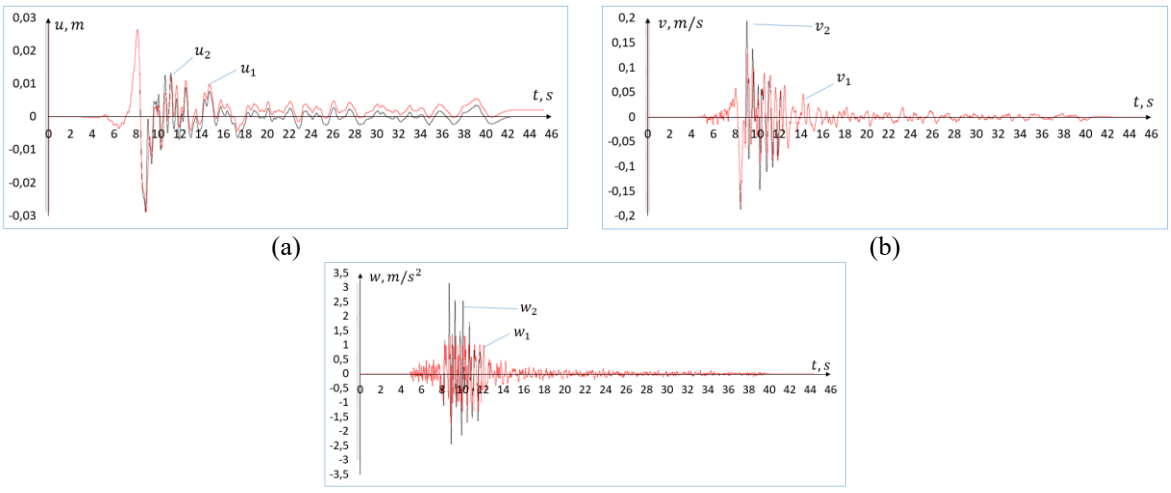

FIGURE 13. Displacements (a), velocities (b), and accelerations (c) of the upper (1) and lower (2) plates at φ=5˚, l=0.01 m.

Figure 14 shows the results obtained for φ=5˚ and l=0 m. In this case u_{1max}=0.029 m, u_{2max}=0.029 m, v_{1max}=0.19 m/s, v_{2max}=0.2 m/s, w_{1max}=1.9 m/s^2, w_{2max}=3.35 m/s^2. The results show that the maximum displacement values are almost identical, the maximum velocity values differ by a factor of 1.1, and the maximum acceleration values differ by a factor of 1.8.

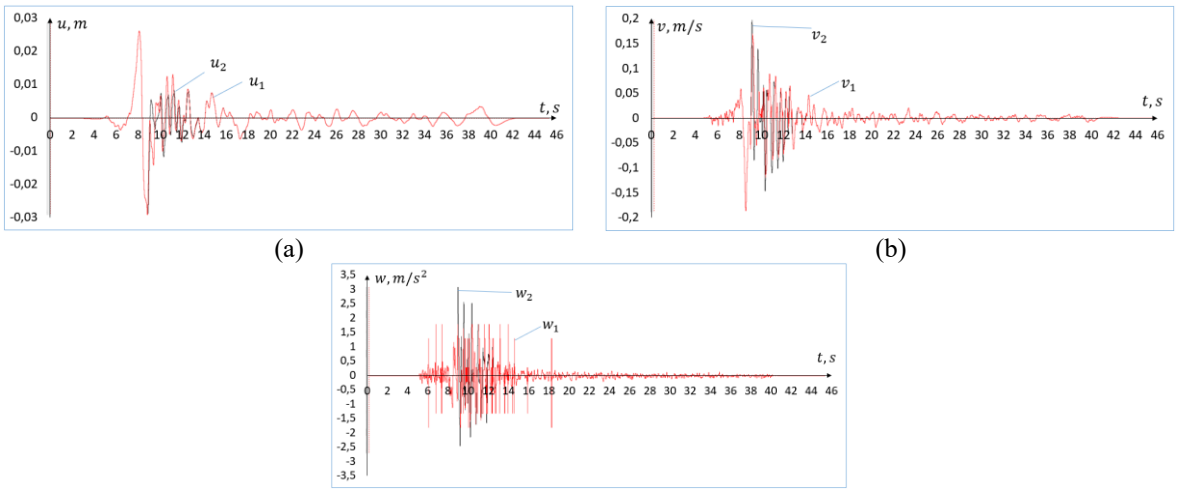

FIGURE 14. Displacements (a), velocities (b), and accelerations (c) of the upper (1) and lower (2) plates at φ=5˚, l=0 m.

The results of the calculations show that the presence of a horizontal section in V-shaped roller isolators significantly reduces the acceleration of the upper plate and, accordingly, increases the effectiveness of the seismic isolator.

CONCLUSION

The plates begin to roll relative to each other only when the inertial force exceeds the sum of all forces acting in the horizontal direction. The seismic isolator may also undergo stick-slip dynamics.

Analysis of the processes in roller sliders has shown that the start of relative movement of the plates and the start of joint movement as a solid body cannot be achieved solely by the function of the difference in speed between the upper and lower plates.

For seismic isolators, it has been established that the presence of a V-shaped bottom plate reduces the effectiveness of the seismic isolator, but allows the top plate to return to its initial position.

The presence of a horizontal flat section in the middle of the V-shaped lower plate of the seismic isolator, which is permissible under the design conditions for buildings and structures, increases its effectiveness.

REFERENCES

1. P.W. Gordon and L.R. Keri, Seismic Isolation for Earthquake-Resistant Structures: A State-of-the-Practice Review. Buildings **2**, 300–325 (2012). https://doi.org/10.3390/buildings2030300
2. M. Hosseini and K. Kangarloo, Introducing Orthogonal Roller Pairs as an Effective Isolating System for Low Rise Buildings. WIT Transactions on The Built Environment, Volume **93**, 151-161 (2007). https://doi.org/10.2495/ERES070151
3. M. Hosseini and A. Soroor, Using Orthogonal Pairs of Rollers on Concave Beds (OPRCB) as a Base Isolation System — Part I: Analytical, Experimental and Numerical Studies of OPRCB Isolators. Struct. Design Tall Spec. Build. **20**, 928–950 (2011). https://doi.org/10.1002/tal.568
4. A.R. Avinash, A. Krishnamoorthy, K. Kamath and M. Chaithra, Sliding Isolation Systems: Historical Review, Modeling Techniques, and the Contemporary Trends. Buildings **12**, 1–23 (2022). https://doi.org/10.3390/buildings12111997
5. A. Kamrava, Seismic Isolators and their Types. Current World Environment, **10**(1), 27-32 (2015). http://dx.doi.org/10.12944/CWE.10.Special-Issue1.05
6. M. Ismail, Seismic isolation of structures. Part I: Concept, review and a recent development. Hormigón y Acero, **69**(285), 147–161 (2018). https://doi.org/10.1016/j.hya.2017.10.002
7. A.P. Norman, D.W. Virden, A.J. Crewe, D.J. Wagg and R.T. Severn, Understanding the dynamics of multi-degree-of freedom structures subject to multiple support earthquake excitation. 13thWorld Conference on Earthquake Engineering, **3324**, (2004).

8. A.A. Taflanidis, A. Giaralis, D. Patsialis, Multi-objective optimal design of inerter-based vibration absorbers for earthquake protection of multi-storey building structures. Journal of the Franklin Institute, **356**(14), 7754-7784 (2019). https://doi.org/10.1016/j.jfranklin.2019.02.022
9. N.A. Ortiz, C. Maglutaa, N. Roitman, Numerical and experimental studies of a building with roller seismic isolation bearings. Structural Engineering and Mechanics, 54(3), 475–489 (2015). https://doi.org/10.12989/sem.2015.54.3.475
10. G.C. Lee, Y.Ch. Ou, Z. Liang, T. Niu and J. Song, *Principles and Performance of Roller Seismic Isolation Bearings for Highway Bridges*. Technical Report MCEER-07-0019, 334 p. (2007). https://doi.org/10.13140/RG.2.2.35091.49447
11. G.C. Lee, Y.Ch. Ou, T. Niu, J. Song and Z. Liang, Characterization of a Roller Seismic Isolation Bearing with Supplemental Energy Dissipation for Highway Bridges. Journal of Structural Engineering, 136(5), (2009). https://doi.org/10.1061/(ASCE)ST.1943-541X.0000136
12. I. Mirzaev and M. Turdiev, Seismic Isolation of NPP Turbine Unit Using Dry Friction Devices. Proceedings of MPCPE 2022, Lecture Notes in Civil Engineering **335**, 53-67 (2023). https://doi.org/10.1007/978-3-031-30570-2_6
13. I. Mirzaev, M.S. Turdiev, The effect of the size of the horizontal gap between the foundation and the sliding grillage on the oscillation of the building during an earthquake. AIP Conference Proceedings **2612**, 040033 (2023). https://doi.org/10.1063/5.0113473
14. I. Mirzaev, Kh. Sagdiev, A. Yuvmitov, M. Turdiev and B.Egamberdiev, Experimental determination of dynamic coefficient of Amonton-Coulomb dry friction. Facta Universitatis Series Mechanical Engineering, **22(3)**, 503– 512 (2024). https://doi.org/10.22190/FUME231225016M
15. M. Roozbahan, Ch. Masnata, G. Turan and A. Pirrotta, Efciency evaluation of optimal TLCD and TMD for the seismic response reduction of buildings considering soil-structure interaction effect. Meccanica, Springer Nature, 11012-025-01981-9, (2025). https://doi.org/10.1007/s11012-025-01981-9
16. T.W. Lin and Ch.Ch. Hone, Base Isolation by Free Rolling Rods Under Basement. Earthquake engineering and structural dynamics, **22**, 261-273 (1993). https://doi.org/10.1002/eqe.4290220502
17. I. Mirzaev J.F. Shomurodov, Wave processes in an extended underground pipeline interacting with soil according to a bilinear model. AIP Conf. Proc **2432**, 030049 (2022). https://doi.org/10.1063/5.0089583
18. S.J. Wang, J.S. Hwang, K.C. Chang, C.Y. Shiau, W.C. Lin, M.S. Tsai, J.X. Hong and Y.H. Yang, Sloped multi-roller isolation devices for seismic protection of equipment and facilities. Earthquake Engineering Structural Dynamics, **43**(10), 1443-1461 (2014). https://doi.org/10.1002/eqe.2404
19. D.N. Nizomov and A.M. Sanginov, Simulation of the interaction of the structure with the foundation under seismic impacts. Bulletin of Science and Research Center of Construction, **3**(38), 143–154 (2023). https://doi.org/10.37153/2618-9283-2023-1-29-37
20. H. Cilsalar and M.C. Constantinou, *Development and Validation of a Seismic Isolation System for Lightweight Residential Construction*. Technical Report MCEER-19-0001, 566 p (2019).